Biaxial pseudodynamic tests of a post-tensioned rocking column with externally mounted energy dissipators

R. Gultom & Q.T. Ma

Department of Civil and Environmental Engineering, The University of Auckland, Auckland, New Zealand.

2015 NZSEE Conference

ABSTRACT: The effects of multi-directional loading during earthquake excitation are often overlooked in laboratory experiments due to the high cost and setup complexity. However many structural failures are caused by the combined effect of multi-directional loading. Currently, there is no definitive guidance on the effects of different displacement tracking objectives on the results of multi-directional physical earthquake simulations. This study tested a post-tensioned rectangular rocking concrete column with externally mounted energy dissipators pseudodynamically subjected to simultaneous biaxial loading. The setup emulated bidirectional earthquake ground motion. The study focused on the effects of different displacement tracking strategies in pseudodynamic tests. Experiments found that different displacement tracking strategies gave rise to additional plastic deformations of the specimen and consequently resulted in appreciable differences in the time history predictions both in amplitude and phase lag. Interestingly, the experiments revealed a design deficiency of the externally mounted energy dissipators. The dissipators were shown to be susceptible to buckle during bidirectional loading, a phenomenon that has been missed in previous earthquake simulations.

1 INTRODUCTION

To date, most experimental seismic simulations only consider uniaxial load action along the principal axes of a specimen. In reality, earthquake loading is multi-directional and most often occur at an oblique angle to a structure's principal axes. Moreover, most structures are irregular and therefore likely to develop torsional responses even under unidirectional earthquake excitation. The importance of including multi-axial effect is further highlighted by the Canterbury Earthquakes experience where many structural failures were attributed to the combined effect of multi-directional loading. Therefore, additional research effort considering multi-axial earthquake load is needed to understand the complex coupled structural responses particularly during inelastic excursions, where stiffness degradation in one axis can significantly affect the same parameter in the other.

1.1 Test specimen and setup

This study conducted biaxial pseudodynamic (PSD) tests on a rocking column. The test specimen was a free-standing concrete column with unbonded post-tensioning (PT) bars and replaceable, externally mounted dissipators (EMD) made from mild steel bars. The PT bars enabled controlled rocking behaviour and the replaceable mild steel bars provided dependable energy dissipations capability during rocking. The structural system was inspired by the PRecast Seismic Structural System (PRESSS) technology which ensured protection against significant structural damage even after a major earthquake event (Priestley et al. 1999). The Alan MacDiarmid building in Victoria University of Wellington, shown in Figure 1 is the first building in New Zealand to adopt such system (BBR Contech 2011).

The unbonded PT column was chosen specifically for this study to allow multiple tests to be conducted on the same specimen with minimum degradation. It is worth mentioning that the test specimen in this series of experiments was similar to the specimens in a previous study by Marriott (2009). The column had a rectangular cross-section (490 × 250 mm) and a cantilever height of 1600 mm. The column had 12 – D10 as longitudinal reinforcements and D10 transverse reinforcements

spaced at 120 mm centers. All reinforcing bars were Grade 300 deformed bars. The column sat atop a concrete foundation block, and the EMD were bolted to the base of the column through a steel brackets. These dissipators were designed to provide energy dissipation as they cycled between tension and compression when the column displaced. Actuators were connected at right angles at the top of the column by means of steel plates and four M25 threaded steel rods. A schematic drawing of the test setup is shown in Figure 2 and photographs of the actual test setup are shown in Figure 3.

Figure 1. The Alan MacDiarmid building, Victoria University of Wellington (left), and close up of the EMD (right) (BBR Contech 2011).

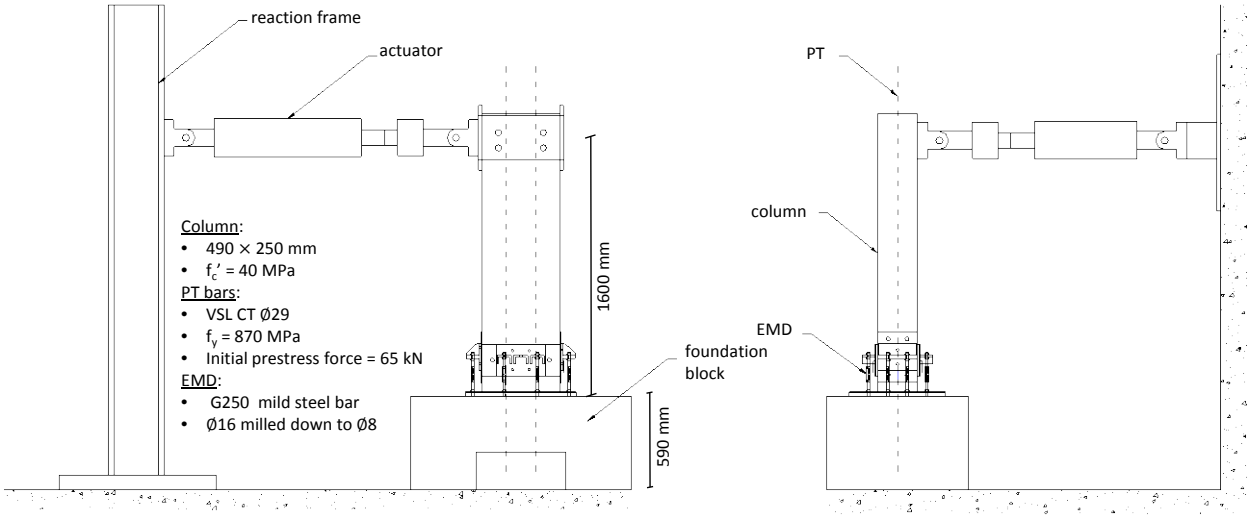

Figure 2. Elevation view of test setup, stronger axis face (left) and weaker axis face (right).

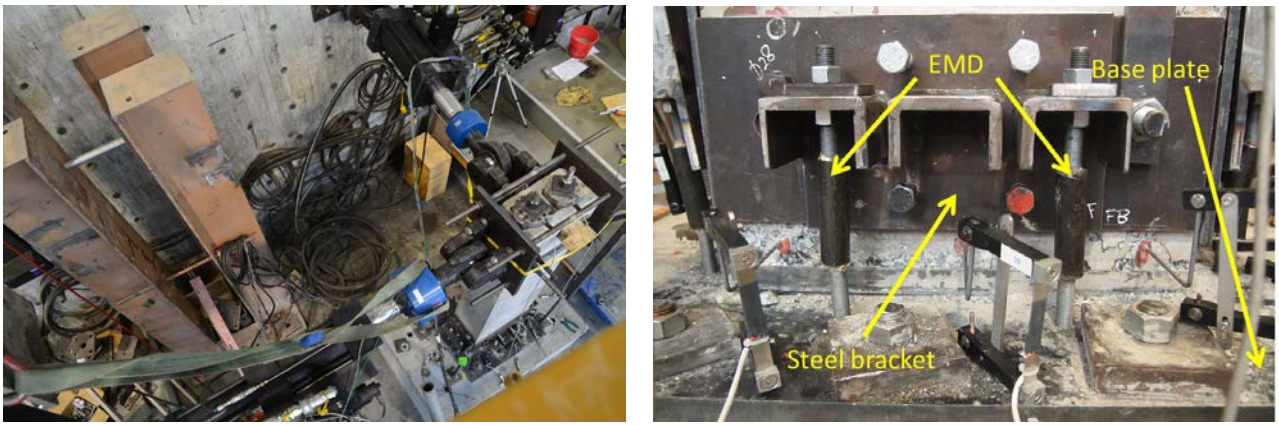

a) b)

Figure 3. Actual experiment setup, a) view from above and b) column base detailing.

1.2 **The pseudodynamic method**

The pseudodynamic (PSD) method subjects a specimen to a displacement history that is determined interactively, according to a numerical model of the system and the measured specimen response during the course of the test. This testing technique is particularly advantageous for seismic simulations as it allows dynamic and inertial effects to be replicated in the numerical model, hence allowing otherwise very large dynamic forces on the physical specimens to be applied at a slower rate or pseudostatically. A description of the basic algorithm is available in Shing and Mahin (1984).

In a 2D application, the column displaces in two transverse directions at the top. The principal axes of the cross section are no longer aligned with the actuator axes due to finite actuator lengths (Figure 4). Therefore an iterative procedure had been developed to account for this geometric error during control signals generation as well as feedback signals processing.

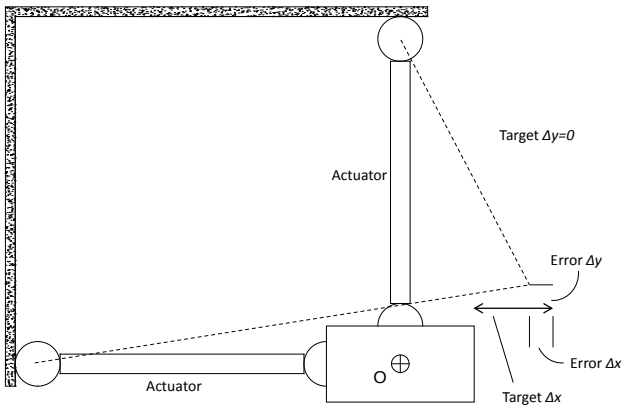

Figure 4. Geometric error in displaced column.

1.3 **Displacement tracking strategies**

Currently, there is no definitive guidance or robust study on the effects of different displacement tracking objectives on the results of multi-directional physical earthquake simulations. It has been shown that different load paths lead to different inelastic load-deformation behaviour of structures (Bousias et al. 1995), and consequently different energy dissipation capability which may not always be proportionally related to the ultimate strength capacity for a given displacement path (Watanabe et al. 2000; Qiu et al. 2002).

For this study, the rocking column was subjected to three patterns of displacement paths in *x*- and *y*-directions during each time step according to the numerical model in the computer. Referring to Figure 5, among infinite possible paths to move the column from Point 1 to Point 2, the experiments adopted a "staggering" pattern. In the first pattern (denoted I in Figure 5), the column was displaced along the stronger axis (henceforth called the *X*-axis) while it was held steady in the weaker axis (henceforth called the *Y*-axis). Afterwards, the column was displaced along the *Y*-axis until Point 2 was reached while the *X*-axis position was held steady. The second pattern (denoted II) was similar to Pattern I except with the order of loading reversed. In the third pattern (denoted III), the column was displaced along both axes simultaneously. Using different displacement tracking for the same earthquake record in a PSD test is analogous to subjecting the structure to a different load path; since the displacement amplitudes the structure is reaching are expected to be the same, the path the structure takes to reach these amplitudes determine how much energy is dissipated.

1.4 **Experiment regime**

The experiment adopted earthquake records that were selected and scaled based on the NZS1170.5:2005 (Standards New Zealand 2004) guidelines for time-history analyses. These records represented the seismicity of the greater Wellington region (Oyarzo-Vera et al. 2012). Figure 6 shows the site-specific target spectra of the assumed region, as well as the pseudo-spectral acceleration (*PSA*) of the scaled earthquake records. The dashed lines indicate the range of periods of interest according to the scaling procedure in NZS1170.5:2005.

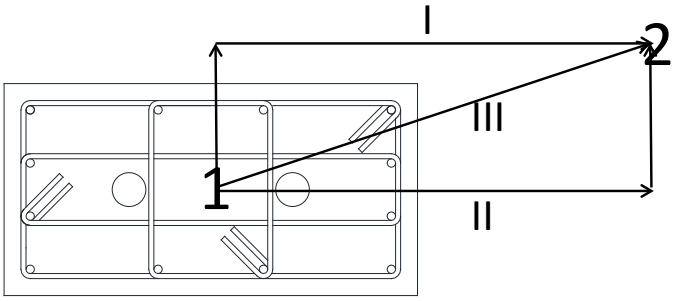

Figure 5. Different displacement paths to a target displacement.

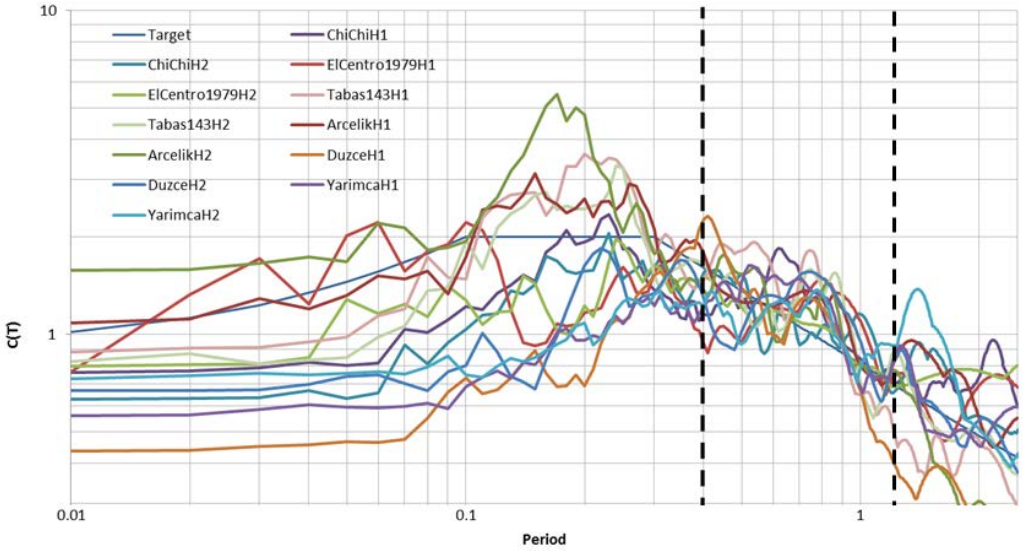

Figure 6. *PSA* of the family of earthquake records used in the testing regime.

a) b)

Figure 7. Buckled EMD, a) during experiment and b) after experiment.

2 RESULTS AND DISCUSSIONS

2.1 EMD failure

There were two factors that probably contributed to the failure of the EMD. The first was the length of the confined portion was shorter than the one tested by Marriott (2009), which could reduce the resistance of the EMD against buckling. The other is the loading regime used in the tests. The biaxial loading at the column led to large bending actions on the EMDs. As the EMD motions were no longer

predominantly axial, on compression cycles following tension cycles, concentrated rotation developed at the junctions where the anti-buckling grouted sleeve terminated. This resulted in significant eccentricity for the axial force and premature failure of the EMD. Figure 7 shows a buckled EMD, the figure highlights that concentrated rotation occurred around the end of the milled-down portion. Although it has been shown through component testing and uniaxial cyclic assemblage test that the EMD yielded dependably in tension and compression (Marriott 2009), it was evident that full performance was not attainable under bi-directional earthquake attack. Preliminary analyses of the experiment results indicated that the EMD failed at about 50% of the intended capacity. It further highlights the importance of considering the effect of multi-axial load on such system.

2.2 **PSD test results**

This section presents the PSD test result from four earthquake records simulations. The PSD tests adopted a 50 times timescale, in other words, a 30-second earthquake record would have taken 25 minutes. Accordingly, the time axes in the following time history plots have been adjusted to reflect the timescale of the actual earthquake. Figure 8 shows the displacement time history and force displacement response of the column from the 1999 Duzce earthquake simulation. Figure 8 highlights noticeable differences in amplitude and phase of the column displacements in both axes due to different displacement tracking strategies. It should be noted that a classical flag-shaped hysteretic curves did not develop, and that appreciable residual drifts were present. This was in part caused by a large crack at one corner of the column and therefore sliding, opening and closing of this crack dominated the hysteretic behaviour. The figure also highlights the poor performance of the EMD due to buckling and slippage. Due to space limitation, other time histories and force-displacement results are not shown but similar trends are also observed.

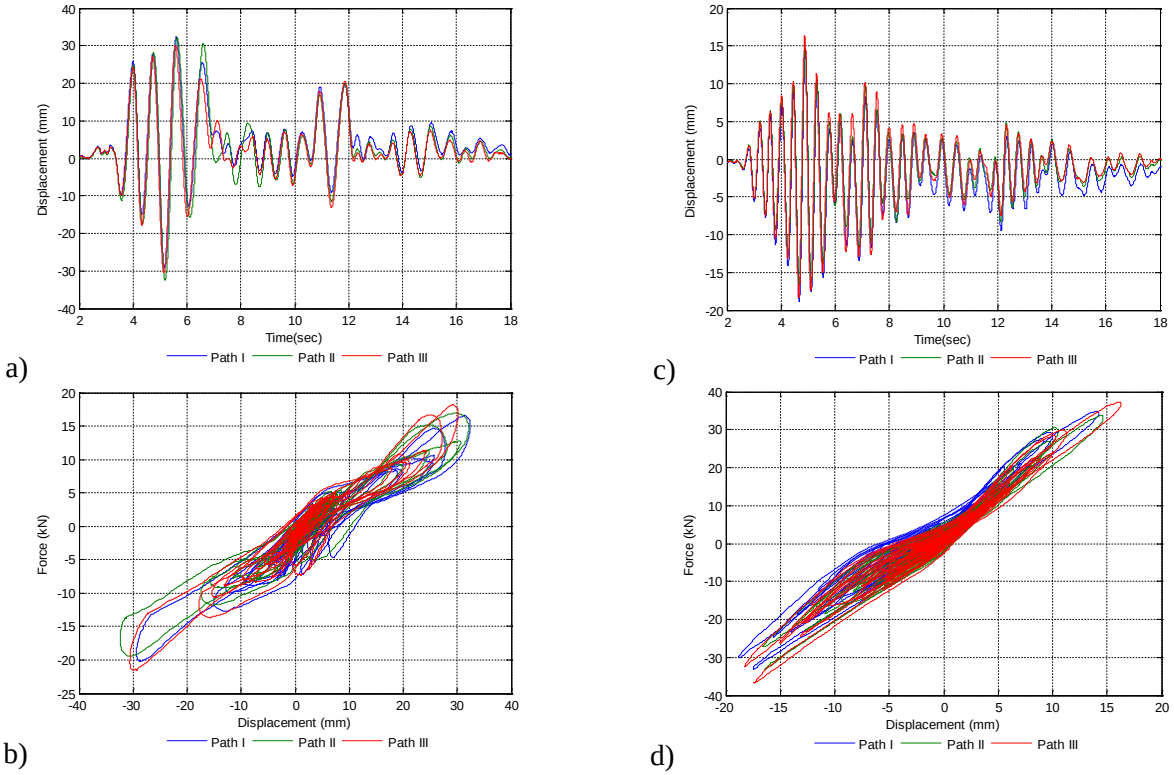

Figure 8. Displacement time history and force-displacement response of the column from the 1999 Duzce earthquake simulation for the weak (a and b) and strong (c and d) axes.

In the absence of true reference result from full dynamic tests (e.g. shake-table test), or idealised numerical simulation, the tracking strategy Path III can be thought as the ideal solution considering the shortest path is the most plausible. For each tracking strategy, the amplitudes attained at every half-cycle in the displacement time history are identified. Figure 9 shows an example of the identified amplitudes, positives and negatives, from the 1999 Duzce earthquake simulation. The amplitudes

attained by tracking strategies Path I and Path II can then be quantified in term of their differences, or errors, relative to Path III. Mathematically, these amplitude differences can be represented as a normalised error ε defined as,

$$\varepsilon_i = \frac{A^i - A^{III}}{A^{III}} \tag{1}$$

In Equation 1, A = amplitude and i = I or II e.g. A^i indicates amplitudes attained during Path i test. Consequently any negative values ε indicate that the attained amplitudes in Path I or II are smaller than the reference value Path III, while positive values indicate the opposite.

Collating the normalised amplitude errors from each cycle in the earthquake time history, Figure 10-13 plot the distributions of these errors as a density function, $f_X(x)$. In each plot, a solid black line parallel with the vertical axis is drawn at zero ε. If different displacement paths, on average, produced the same amplitudes displacement, this would be indicated by the peak (median) of the density function coinciding with this line. It is interesting to note that the median values of ε across all results are mostly positive, i.e. the amplitudes at peaks of each cycle attained via Path I and II are generally larger than Path III. During Path I or Path II tests, the column displaced a greater distance compared to Path III, providing greater opportunity for increased plastic deformation in the column. Therefore it is likely that the column developed a lower restoring force which in turn led to larger displacement in the PSD algorithm.

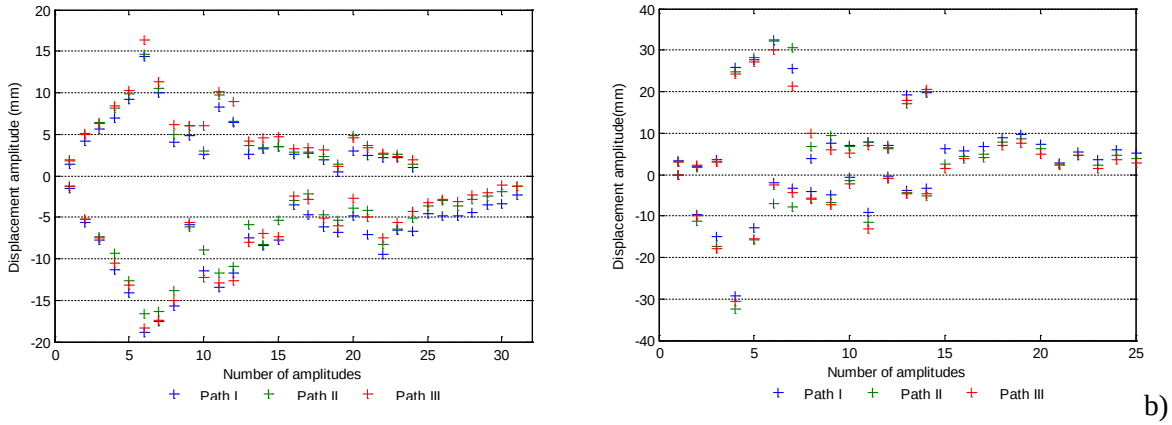

a) b)

Figure 9. Displacement amplitudes attained during the 1999 Duzce earthquake (Duzce, Turkey) simulation, a) *X*-axis and b) *Y*-axis.

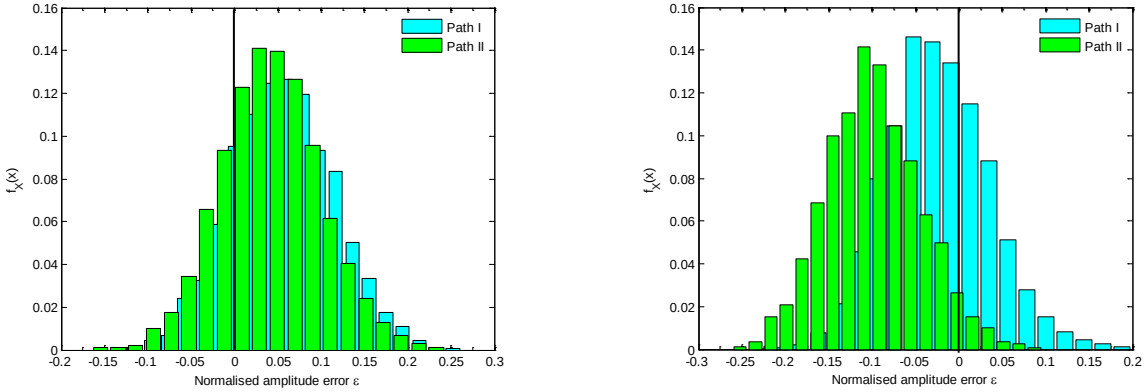

a) b)

Figure 10. Distribution of normalised amplitude errors from 1979 Imperial Valley earthquake simulation, a) *X*-axis and b) *Y*-axis.

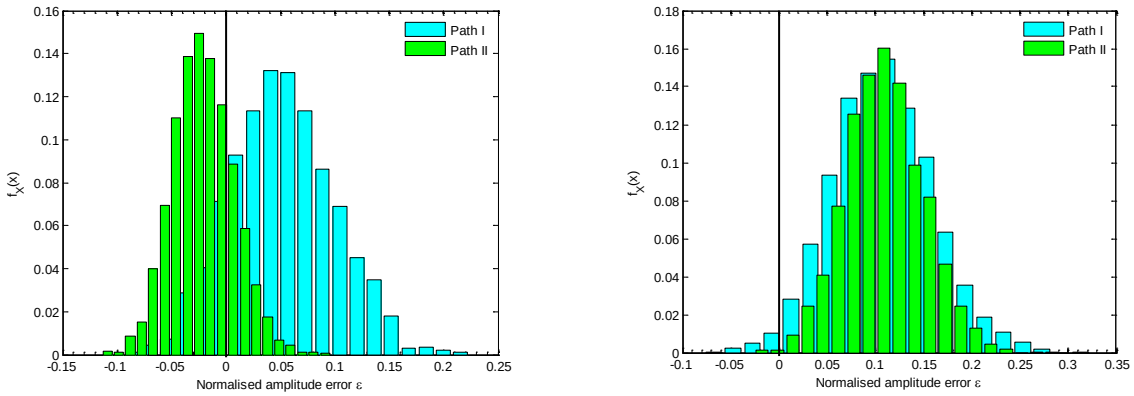

a) b)

Figure 11. Distribution of normalised amplitude errors from 1999 Duzce earthquake (Duzce, Turkey) simulation, a) *X*-axis and b) *Y*-axis.

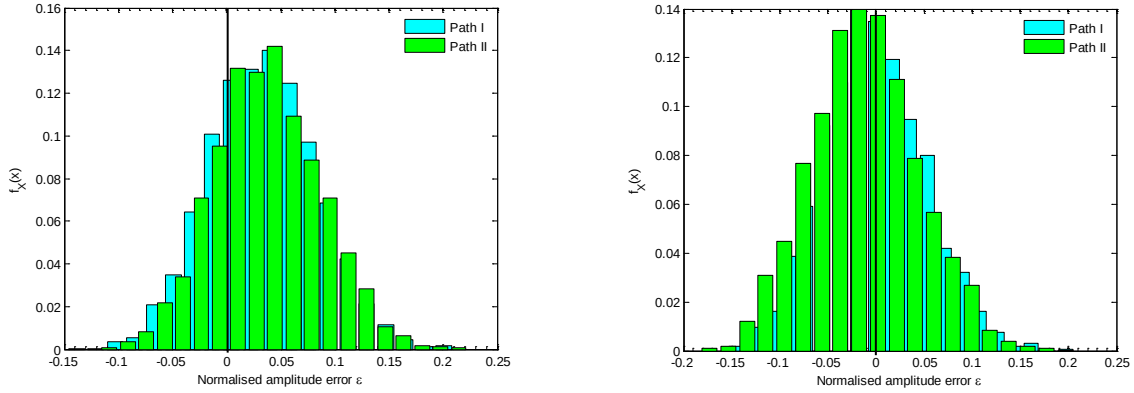

a) b)

Figure 12. Distribution of normalised amplitudes errors from 1978 Tabas earthquake (Tabas, Iran) simulation, a) *X*-axis and b) *Y*-axis.

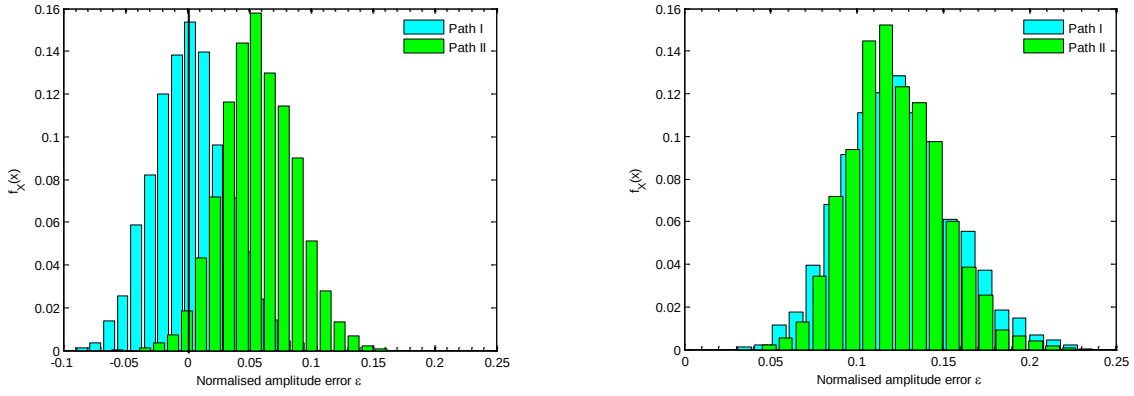

a) b)

Figure 13. Distribution of normalised amplitudes errors from 1999 Yarimca earthquake (Kocaeli, Turkey) simulation, a) *X*-axis and b) *Y*-axis.

3 CONCLUSION

This study on a rocking column has shown that different displacement paths in bidirectional earthquake simulations led to different results, particularly when inelastic response is expected. This phenomenon occurs in quasi-static tests as well as PSD simulations. Three displacement tracking strategies were tested in this study. The resulting error distributions suggest that different displacement tracking strategies led to noticeable differences in the displacement amplitudes attained by the specimen. The experiments also exposed failure of the externally mounted dissipator during testing where the dissipators buckled prematurely under bidirectional loading. While the biaxial loading regime used in the study is definitely a contributing factor, the insufficient length of the confined region of the EMD is probably another factor. Improvement in the design should be verified through more biaxial experiments.

4 ACKNOWLEDGEMENT

The authors wish to thank the Earthquake Commission for the financial support of this project through the Biennial Research Funding Programme, project BIE12/632.

5 REFERENCES

BBR Contech. 2011. VUW PRESSS Building. Retrieved 5 February, 2015, from http://contech.co.nz/uploaded/VUW%20Alan%20MacDiarmid%20PRESSS%20Building.pdf.

Bousias, S.N., Verzeletti, G., Fardis, M.N. & Gutierrez, E. 1995. Load-path effects in column biaxial bending with axial force. *Journal of Engineering Mechanics* 121(5): 596-605.

Marriott, D.J. 2009. The development of high-performance post-tensioned rocking systems for the seismic design of structures *PhD Dissertation*, University of Canterbury.

Oyarzo-Vera, C.A., McVerry, G.H. & Ingham, J. M. 2012. Seismic zonation and default suite of ground-motion records for time-history analysis in the North Island of New Zealand. *Earthquake Spectra* 28(2): 667-688.

Priestley, M., Sritharan, S., Conley, J.R. & Pampanin, S. 1999. Preliminary results and conclusions from the PRESSS five-story precast concrete test building. *PCI journal* 44(6): 42-67.

Qiu, F., Li, W., Pan, P. & Qian, J. 2002. Experimental tests on reinforced concrete columns under biaxial quasi-static loading. *Engineering structures* 24(4): 419-428.

Shing, P.B. & Mahin, S.A. Pseudodynamic test method for seismic performance evaluation: theory and implementation. *Report No. UCB/EERC-84/01* (University of California, Berkeley, California, 1984).

Standards New Zealand 2004. Structural Design Actions. *Part 5: Earthquake actions – New Zealand*. Wellington, New Zealand.

Watanabe, E., Sugiura, K. & Oyawa, W.O. 2000. Effects of multi-directional displacement paths on the cyclic behaviour of rectangular hollow steel columns. *Structural Engineering/Earthquake Engineering* 17(1): 69-85.